

# Multiphase Fluid Hammer in Propellant Lines

Lema, M.\*†, Porca-Belío, P.\*, Steelant, J.‡, López-Peña, F.† and Rambaud, P.\*

\* von Karman Institute for Fluid Dynamics, 1640 Rhode-St-Genése, Belgium

† University of A Coruña, 15000 A Coruña, Spain

‡ ESTEC-ESA, 2200 AG Noordwijk, The Netherlands

The priming operation in a spacecraft propulsion system involves adverse fluid hammering effects and several multiphase phenomena, such as cavitation, boiling front and absorption and desorption of a non condensable gas. Due to the lack of detailed experiments in the literature, the physical models implemented in the numerical codes cannot be validated properly and they fail when computing the priming process. The aim of this study is to model experimentally the spacecraft's hardware, in order to build an experimental database for the validation of numerical codes. This paper describes the experimental facility designed to reproduce the priming operation and shows preliminary results obtained with a simplified test bench, built for assessment of the experimental procedure. The comparison of the experimental results against computations with EcosimPro/ESPSS shows an acceptable agreement.

## Introduction

The operation of spacecraft propulsion systems is regularly faced with adverse fluid hammering effects during the priming operation. This maneuver is done by fast opening of a pyrotechnic isolation valve and a latch valve, which results in the filling and pressurization of the propellant lines of the spacecraft. This operation may turn out to be critical if the corresponding over-pressures are not correctly taken into consideration in the pipe line and sub-system dimensioning. Furthermore, since the propellant lines are initially vacuum pumped or filled with a non-condensable gas, the classical water hammer includes various multi-phase phenomena, such as cavitation and boiling front. On top of that, the propellant is pressurized in the tanks by means of a driving pressure gas, which can be absorbed into the liquid propellant during storage. Depending on the absorption rate, the speed of sound of the liquid phase can change and the pressurant gas can desorb during the priming process.

Today's numerical models of the fluid hammer phenomenon in fluid networks are established on the basis of results obtained with water in simple configurations. Due to the complexity of the multiphase phenomena occurring in spacecraft hardware, there are very few literature references describing experiments with all the specifications of the above configuration, which are necessary for a proper validation of the physical models implemented in the simulation tools. Nowadays, various numerical codes are able to accurately predict the effects of liquid compressibility when computing a single-phase fluid hammer but they still need to be extended and calibrated for cases with cavitation (single component) and two-phase (two-component) flow. Furthermore, the treatment of a dissolved non-condensable gas in the liquid phase needs to be improved. In both cases, the existence of a well documented experimental database is mandatory for the improvement and validation of the physical models currently available for the fluid hammer prediction.

This study proposes an experimental and numerical investigation of the fluid hammer phenomenon in a confined environment. The experimental approach come to complete the few references available in the literature modeling the spacecraft's hardware, [1] and [2], but using an experimental setup which can reproduce all the physical phenomena taking place in the propellant lines during the priming process.

This paper describes first the experimental facility and the difficulties encountered during the design process. The experimental set-up aims to reproduce the priming process in the laboratory for different propellant lines configurations. Furthermore, a simplified facility has already been built and tested in order to assess the experimental procedure. The experimental measurements obtained with this simplified facility are shown, together with a first comparison against EcosimPro calculations.

## Facility design

The facility will be designed based on the same conception rules than the satellites. Therefore, one must first review the hardware configuration and all the physical phenomena involved in the real propellant system during priming. Prior to the priming operation, the propellant lines are vacuum pumped ( $P < 1$  kPa) and/or filled with a non-condensable gas (N<sub>2</sub> or He), which is also used to pressurize the propellant tank at 20 bar. There is an amount of the pressuring gas in the tank that will be dissolved in the liquid propellant (monomethylhydrazine, MMH, or Dinitrogen Tetroxide, NTO) and, according to Henry's law, the quantity of the dissolved gas is proportional to the partial pressure of the gas in equilibrium with the liquid for a given temperature and pressure. Depending on the absorption rate, the speed of sound of the liquid phase can change.

During priming, the pyrotechnic valve is fast opened in less than 5 ms and the latch valve in less than 30 ms, filling with propellant the line till the flow control

valve. This operation induces a fluid hammer pressure front with a pressure surge in the flow that might exceed 250 bar. Besides, the pressure that the front sees in the pipe can be below the vapour pressure of the propellant resulting in a cavitation regime and a boiling front, where the one-phase flow is transformed to two-phase flow. On top of that, the gas absorbed during storage can desorb in the pipe, where the initial pressure is below the equilibrium pressure, and can be absorbed again when the pressure front impacts against the flow control valve. Finally, there is also the Fluid-Structure Interaction (FSI) due to the increase of the pipe cross section at the water hammer front location. The inertial displacement of the pipe may result into a cavitation bubble of vapor with column separation. The bubble collapse may cause another rise in pressure. The pipe deformation and any other fluid structure interaction depend on the material Young's modulus and on the pipe wall thickness. FSI should be avoided in the experimental measurements due to the known difficulties to characterize concurrently waves travelling in the liquid and in the solid. Furthermore, in this study and for validation purposes it is preferred to increase the rigidity of the experimental system in order to obtain unambiguous measurements that will be compared with simulations having simpler boundary conditions, i.e., without accounting numerically for wall deformation.

To model experimentally the priming operation, the facility has to include the elements directly involved in the fluid hammer occurrence, i.e. the propellant tank, a fast opening valve, and a given length of the propellant line with different configurations, referred as test elements hereafter. Furthermore, the set-up will include a vacuum system to set the experiment's initial conditions, a purge to fill the line with a non-condensable gas, and a feeding valve to inject the working fluid into the tank, as sketched in figure 1.

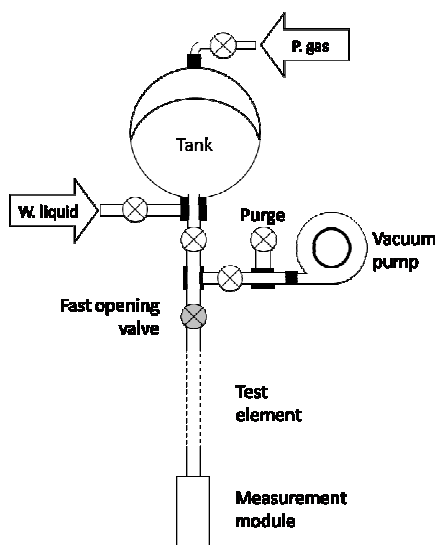


Figure 1. Facility layout.

The design is flexible enough to study different test elements configurations, such as simple straight pipe, two straight pipes connected by a 90° elbow and one straight pipe mounting a T-bifurcation. These flexibility

in the configuration will allow to isolate and to study the effect of an elbow and a bifurcation on the pressure wave generated by the fluid hammer. All the configuration will be made with titanium tube with the standard diameter used by the aerospace industry, that is to say 1/4 inches. The test liquids are inert fluids such as water, acetaldehyde, ethanol, isopropyl alcohol (IPA) and hydrofluoroether (HFE) instead of the highly toxic real propellants; MMH and NTO.

The pressurized tank acting as a propellant is a spherical accumulator, with the advantage of mounting an elastic membrane to avoid the contact of the test liquid with the pressurant gas. This solution allows running experiments without absorption of the pressurant gas in the liquid. These test results will provide very useful insights to understand how the dissolved gas affects the fluid hammer mechanism. Moreover, in order to run experiments with a working fluid free of dissolved gas, the working liquid needs to be deaerated, as it is already saturated with air in standard conditions. The deaeration process is done by means of a depressurization process using a second accumulator, called pre-tank in figure 2, connected to a vacuum pump. The dissolved gas is removed by keeping the liquid in a vacuum atmosphere enough time. Once the deaeration is done, the liquid is pushed towards the main tank by injecting compressed air in the gas side of the accumulator. Thanks to the membrane that mounts the pre-tank, the liquid is not in contact with any gas during the transvasation operation.

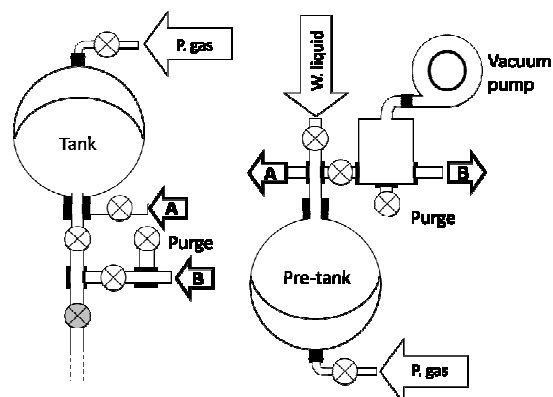


Figure 2. Facility layout including the deaeration system.

The layout of figure 1 and 2 is intent to be clamped on a vertical wall. This orientation is proposed vertically in contrast with recent studies on the same subject, references [1] and [2], where the fluid hammer reflected waves were travelling in a horizontal test element, together with a vertical tube connecting the test element with the tank (see figure 4 obtained from [1]). It is believed that the cancelation of singular elements such as 90° elbows and T-junction upstream of the latch valve will improve not only the measurements, but also the numerical simulation and the general interpretation of the pressure signal. Indeed, these elements are suspected to modify the amplitude and frequency of the different pressure. Furthermore, the simpler is the configuration, the easier is to control the fluid structure interaction. Nevertheless, the facility will be designed and installed in such a way that it will be possible to go

from a fully vertical configuration to a vertical/horizontal configuration similar to the one sketched in figure 3.

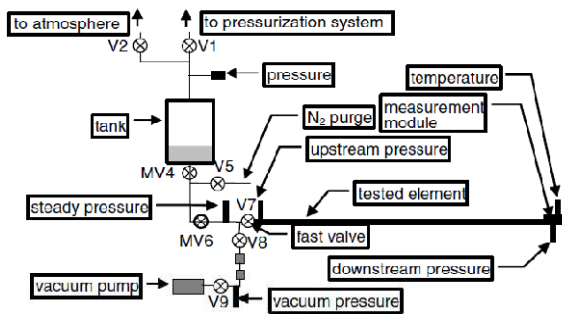


Figure 3. Facility layout built in ONERA [1]

Finally, in figure 4 is shown the final design of the experimental facility. The right side of the drawing shows the deaeration system, which includes the vacuum pump, the membrane accumulator and the decanting vessel to avoid liquid flowing into the pump. The main elements of the facility are mounted on a thick steel platform, which in turn is rigidly clamped on a concrete wall. On the upper part of the platform is placed the tank, which has been modified to fit the ultrasonic transducer. The tank outflow is connected to the fast opening valve by several piping elements with  $\frac{1}{2}$  inch of internal diameter. This fact makes necessary to use a convergent element after the valve, since the test element has a diameter of  $\frac{1}{4}$  inch. In this study, two types of fast opening valves will be used: a solenoid seat valve and a ball valve with a mechanical actuators. Both ensure opening times equal or below 30ms. Finally, a measurement module is attached at the end plug of the test element,

### Measurement techniques

Regarding the measurement techniques, one can distinguish two groups. The first group includes the necessary transducers to set and monitor the experiment's initial conditions, i.e. speed of sound, temperature and pressure of the test fluid in the tank, and vacuum level in the test element. Temperature is measured with type K thermocouples and pressure with differential pressure transducers. The tank is equipped with an ultrasonic transducer in order to measure the speed of sound in the liquid, while the liquid is pressurized prior to launch the test. This measurement allows characterizing the influence of the absorption and desorption rates of the pressuring gas on the speed of sound.

The second group of transducers corresponds to the necessary measurement techniques to properly record the wave front induced by the fluid hammer at the impact location, including fast response, unsteady pressure and temperature transducers in the measurement module, which is attached to the plug end as sketched in figure 5. Pressure is measured with piezoelectric sensors and temperature with coaxial

thermocouples, type E, both with response frequencies higher than 50 kHz. All the transducers are flush mounted in the measurement module.

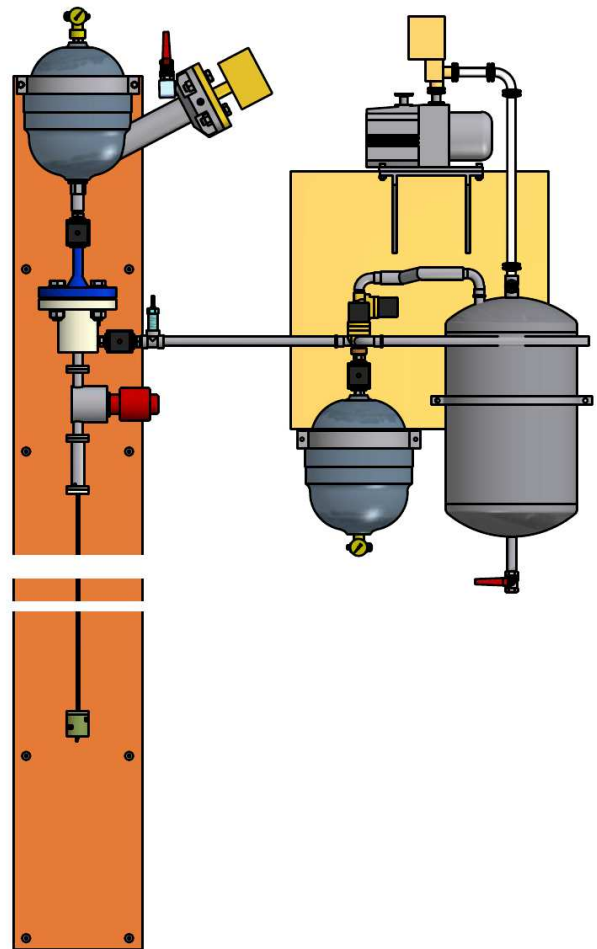


Figure 4. Final design of the facility

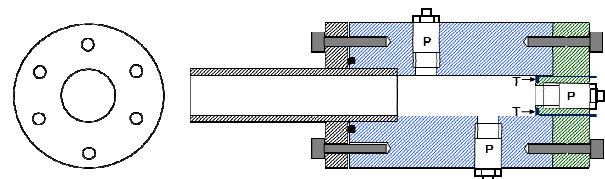


Figure 5. Instrumented measurement module attached to the downstream impact end.

An unsteady pressure transducer is also mounted right after of the fast opening valve and, when correlated with the ones mounted on the instrumented measurement module, will make possible to determine the travelling velocity of the wave front. This value may differ from the speed of sound in the liquid measured by the ultrasonic transducer, due to the desorption rate of the pressuring gas during the fluid hammer process.

There is a second interchangeable module proposed in this study made out of quartz. This transparent module will be dedicated to flow visualizations with high speed imaging. The aim of these measurements is to characterize the liquid front progression, checking the existence of a boiling front.

## Experimental results

At the time this paper is being written, the construction of the facility described above has not been completed and as a consequence, no experimental measurements can be shown at this stage. Nevertheless, a preliminary setup has been built to help in the design of the main facility. This setup is a simplified version of the one described above, using a simple tank, a ball valve with pneumatic actuator, which is fully opened in 300 ms, and a measurement module with a single unsteady pressure transducer flush mounted at the bottom end. The maximum working pressure of the transducer is 35 bar. The test element consists of a 2 m long straight pipe and internal diameter 12,5 mm. The complete piping network is made with carbon steel tubes and mounted horizontally, as sketched in figure 6. The working liquid is water and the driving pressure gas is air.

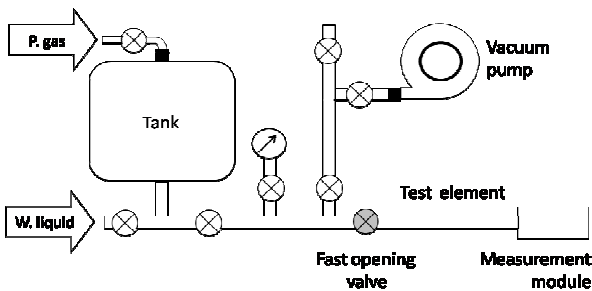


Figure 6. Layout of the simplified facility

Due to the limitation in pressure of the transducer used in this study, the highest pressure in the tank was limited to 4 bar in absolute scale. The preliminary experimental campaign follows the test matrix displayed in the Table 1:

		$P_{\text{pipe}}$ [kPa]		
		10	25	50
$P_{\text{tank}}$ [bar]	4	Test 1	Test 2	Test 3
	3,5	Test 4	Test 5	Test 6
	3	Test 7	Test 8	Test 9

Table 1: Test matrix

Every test condition has been repeated two times in order to check the repeatability of the physical phenomenon. The unsteady pressure measurements consist of 500.000 sample points with an acquisition rate of 100 kHz.

The graphs plotted in figures 7, 8 and 9 show the pressure surge evolution for different initial “vacuum” conditions in the test element. For all these tests, the tank pressure was kept constant. As expected, one can see that decreasing the initial pressure in the pipe results in higher pressure surge caused by the wave front reaching the end of the test element.

For the different tests at a constant tank pressure, it is noticed that the time delay between the valve opening and the first pressure surge is slightly increasing when the initial pressure in the test element is higher.

Furthermore, the time delay between the first peak and the second peak is also found dependant to the initial pressure in the test element. The intensity of the first peak is directly related to the pressure difference between the tank and the test element. According to the Joukowsky’s relation, the pressure surge intensity is proportional to the product between the liquid density, the speed of sound in the liquid and the velocity of the liquid front. The increasing time delay between the valve opening and the first peak when the initial pressure difference decreases may be associated to a lower liquid velocity front. This lower velocity, according to the Joukowsky’s relation, will also results in lower first peak intensity. The increasing time delay between the first peak and the second peak, together with the broadening of the second peak is due to a weaker speed of sound in the liquid when the test element is not totally vacuumed. As a matter of fact, the residual air that is compressed by the liquid front may be absorbed in the liquid or may appear as a two-phase mixture having a lower speed of sound.

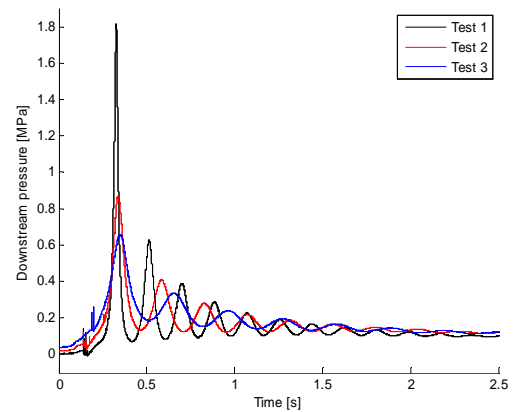


Figure 7.  $P_{\text{tank}}=4$  bar, test 1  $P_{\text{pipe}}=10$  kPa, test 2  $P_{\text{pipe}}=25$  kPa, test 3  $P_{\text{pipe}}=50$  kPa

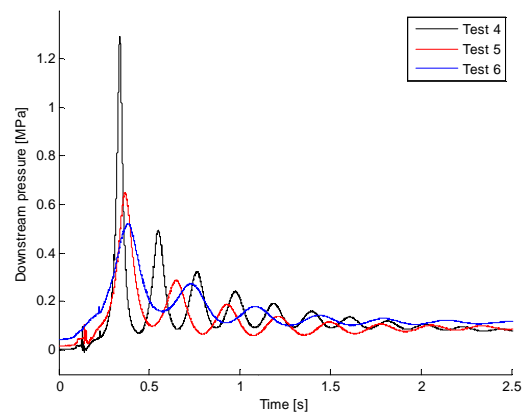
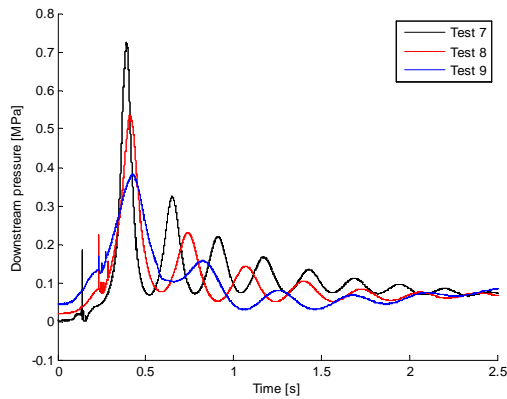


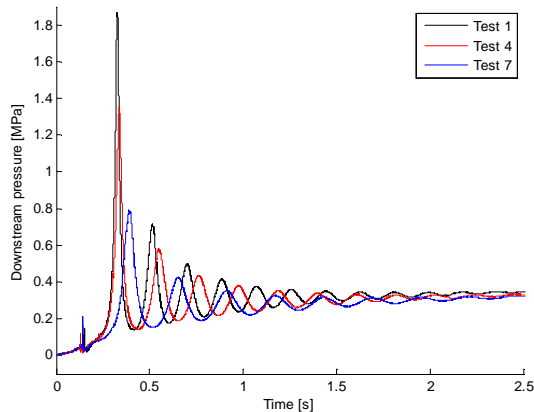
Figure 8.  $P_{\text{tank}}=3,5$  bar, test 4  $P_{\text{pipe}}=10$  kPa, test 5  $P_{\text{pipe}}=25$  kPa, test 6  $P_{\text{pipe}}=50$  kPa

Figure 10 shows the pressure evolution for the three experiments with the same initial pressure in the pipe but with different pressures in the tank. According to this graph, the pressure surges are higher when the pressure in the tank increases, in the same way that when the initial pressure in the pipe decreases. One may question if the pressure surge depends more on the initial pressure in the pipe or on the pressure in the tank.



**Figure 9.**  $P_{\text{tank}}=3,5$  bar, test 7  $P_{\text{pipe}}=10$  kPa, test 8  $P_{\text{pipe}}=25$  kPa, test 9  $P_{\text{pipe}}=50$  kPa

The graph plotted in figure 11 tries to answer this question by plotting the ratio of the maximum peak pressure to the tank pressure in the Y-axis against the tank pressure in the X-axis. Points with the same colour represent tests with the same initial pressure in the pipe. When the pressure in the pipe is 25 kPa and 50 kPa, the evolution of the maximum pressure peak follows the same slope. On the contrary, decreasing the pressure in the pipe up to 10 kPa results in a more abrupt increase on the pressure surge, showing that decreasing the initial pressure in the tank has a stronger influence on the fluid hammer occurrence.



**Figure 10:**  $P_{\text{pipe}}=10$  kPa, test 1  $P_{\text{tank}}=4$  bar, test 4  $P_{\text{tank}}=3,5$  bar, test 7  $P_{\text{tank}}=3$  bar

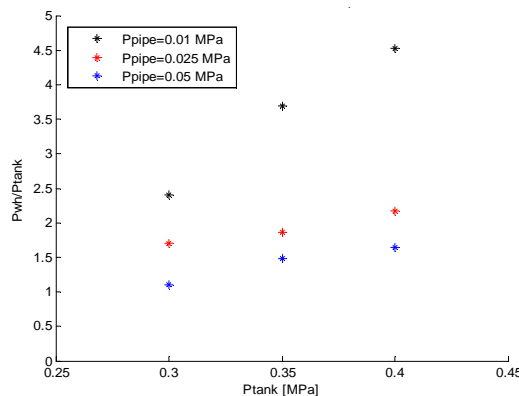


**Figure 11.** Ratio of the maximum peak pressure to the tank pressure against the tank pressure

## EcosimPro simulations

Preliminary computations of the simplified facility have been performed with the numerical tool EcosimPro in a first attempt to compare the simulation results against the experimental data. EcosimPro is a 1D simulation tool, object-oriented and capable of computing both steady state and transient physical phenomena. The calculations are carried out using the European Space Propulsion System Simulation (ESPSS) library, that consists of multiple libraries to represent a functional propulsion system, i.e. fluid properties, multi-phase fluid flow, two-phase two fluids tanks, etc.

Based on the simplified test set-up shown in figure 6, the model on EcosimPro was done with generic objects from the ESPSS library [4] and respecting the real dimensions. The EcosimPro schematic view of the set-up is plotted in figure 12.



**Figure 12.** Schematic view of the experimental set-up under EcosimPro.

In figures 13, 14 and 15 is plotted the comparison of the numerical data against the experimental results obtained for three test cases. The graphs show a reasonably good agreement: in test 1 (figure 13) a similar first pressure peak is obtained, but EcosimPro over predicts this first peak with the other test conditions (shown here only test 2 and 3 in figures 14 and 15). The successive pressure spikes are always higher in the computations. The time delay between peaks is nearly identical and the damping for the second pressure peak is also very consistent with the experimental data. Even if these results are very promising, this comparison will have to be improved in the future when the pressure loss in the valves is known, which is not the case in this preliminary facility, and when the dissolved gas or the two-phase effects on the speed of sound in the liquid is correctly characterized.

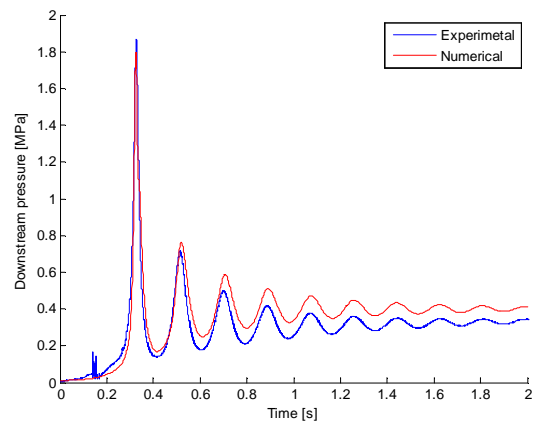


**Figure 13.** Comparison of the experimental data with EcosimPro. Test 1:  $P_{\text{pipe}}=10$  kPa,  $P_{\text{tank}}=4$  bar

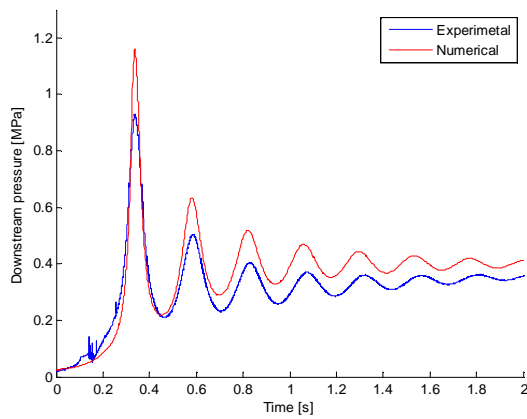


**Figure 14.** Comparison of the experimental data with EcosimPro. Test 2:  $P_{\text{pipe}}=25 \text{ kPa}$ ,  $P_{\text{tank}}=4 \text{ bar}$

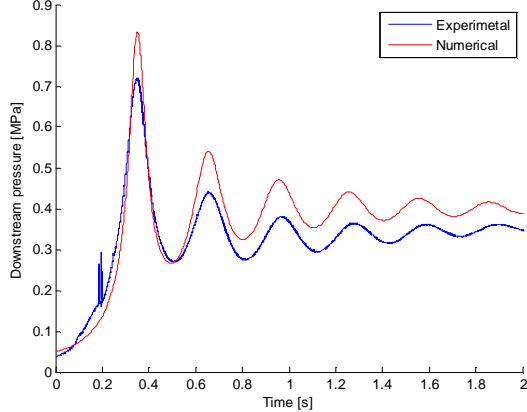


**Figure 15.** Comparison of the experimental data with EcosimPro. Test 3:  $P_{\text{pipe}}=50 \text{ kPa}$ ,  $P_{\text{tank}}=4 \text{ bar}$

As a matter of fact, reference [3] reports validation of EcosimPro against experimental data with a better agreement than the first attempt presented here. Indeed in the present campaign, the pressure history measured at the end plug presents a first raise followed by a small plateau; the plateau is followed by a small pressure drop prior to the continuous raise of the pressure (see figure 14). This behavior was observed with all the test conditions, but it is more important when the initial pressure in the pipe is 50 kPa or 25 kPa. Such complex behavior may be explained in a space-time diagram of pressure with the path of the different compressing waves in the residual air, its reflection on the end plug, the liquid front wave and all the wave interactions. All this complexity in the pressure signal is not observed in the numerical results and which would explain why the first pressure peak is lower in the experiments compared to the computation when the initial pressure in the pipe is increased. This fact makes the authors to believe that improvement in the modeling is necessary, mainly in the liquid-gas mixing process. As a comparison, in reference [3] the tests were performed with initial pressures in the pipe in the vicinity of 1 kPa, and with a test pipe of 5,54 mm of internal diameter, compared to 12,5 mm in our facility and more than 10 kPa in the pipe. Thus the amount of remaining gas in the pipe is not negligible from an experimental point of view in the present facility.

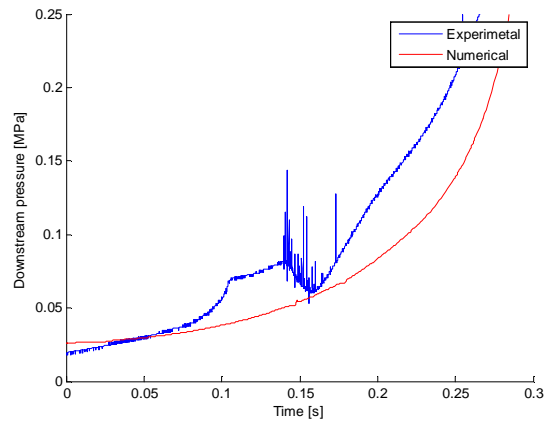


**Figure 16.** Beginning of the pressure surge for test 2

This simplified study presents several aspects that are not correctly assessed yet. First of all, the pressure loss in the valves are not measured, nor estimated correctly. The absorption of the pressuring gas in the liquid is also unknown and the two-phase character of the mixing is not correctly documented. Finally, there is a considerable fluid structure interaction (FSI), which causes the vibration of the whole facility during the test, which attenuates the pressure surges. Unfortunately, we cannot clamp more rigidly the facility in order to check if the FSI is enough to damp so effectively the fluid hammer. We have to remind to the reader that the aim of this simplified facility was to validate the experimental procedure and not to conclude a proper validation. This will be achieved with the facility described in the “Facility design” section, where all these uncertainties will be avoided and all the boundary conditions will be clearly defined.

## Conclusions

This paper describes the design of a new experimental facility to study the fluid hammer occurrence modelling the priming process in spacecrafts. The measurement techniques include the characterization of all the multiphase phenomena related to the fluid hammer occurrence, together with unsteady measurement of pressure and temperature and flow visualization. The assessment of the experimental procedure has been done with a simplified test facility and the experimental data obtained was compared with EcosimPro/ESPSS calculations. The overall comparison is good, even if there is an over estimation of the pressure surges in the calculations. It is believed that the remaining gas in the test element may decrease the first pressure peak produced by the fluid front and other related two-phase flow effects. With the new facility, the experimental results should be more reliable, offering a better validation of the computations.

## References

- [1] Lecourt R. and Steelant J., *Experimental Investigation of Water Hammer in Simplified Feed Lines of Satellite Propulsion Systems*, J. of Propulsion and Power, Vol. 23(6), pp 1214-1224, 2007

[2] Gibek I., Maisonneuve Y., *Waterhammer Tests With Real Propellants*, AIAA paper 2005-4081, Joint Propulsion Conference and Exhibit, Tucson, July 2005.

[3] Christophe Koppel, Jose Moral, Marco de Rosa, Ramon Perez Vara, Johan Steelant and Pierre Omaly, *A Satellite Platform Modelling with EcosimPro: Results of the Simulation Compared to the Ground Tests*. SimTecT 2009 Simulation Conference, Adelaide, Australia, 15 - 18 June, 2009

[4] J. Moral, R. Pérez Vara, J. Steelant and M. de Rosa, *ESPSS Simulation Platform*. 2010 Space Propulsion conference, San Sebastián, Spain, 3 – 6 May, 2010

Contact: [lema@vki.ac.be](mailto:lema@vki.ac.be)